POWER OPTIMIZATION MANAGEMENT FOR LOW-VOLTAGE DISTRIBUTION NETWORKS WITH HIGH-PENETRATION DISTRIBUTED PHOTOVOLTAICS AND ENERGY STORAGE SYSTEMS

Jie LI[12*], Minglin WANG[3], Wei LAI[4]

To address challenges in improving renewable energy utilization efficiency and mitigating node overvoltage issues caused by high-penetration distributed photovoltaic (PV) integration in low-voltage distribution networks (LVDNs), while enhancing voltage security margins, this paper proposes a multi-objective optimization model and power management strategy for LVDNs integrated with distributed PV and distributed energy storage systems (DESS). Four comprehensive simulation cases validate the proposed approach. Results demonstrate that this method effectively maintains node voltages within permissible limits while ensuring the economic operation of LVDNs.

Keywords: distributed PV; LVDNs; DESS; power optimization management

Nomenclature for Equations (6) and (6')

Symbol	Description
t	Time interval index
T	Total number of time intervals
Δt	Duration of a time interval
N_B	Number of DESS
M_1	Number of PV sources (indexed by i)
N	Number of load points
$p_g(t)$	Active power at PCC (kW)
$q_g(t)$	Reactive power at PCC (kVar)
$p_i(t)$	Active power of i-th PV (kW)
$q_i(t)$	Reactive power of i-th PV (kVar)
$p_{B,i}(t)$	Active power of i-th DESS (kW; +discharging, -charging)
$q_{B,i}(t)$	Reactive power of i-th DESS (kVar)

[1] Prof., Chongqing Electric Power College, Chongqing, China, e-mail: LiJiecqu@hotmail.com;
[2] Prof., Chongqing College of Mobile Communication, Chongqing, China, e-mail: LiJiecqu@hotmail.com
[3] Eng., State Grid Shandong Electric Power Company Weifang Power Supply Company, Weifang, China, e-mail: 18996300667@163.com
[4] Associate Prof., State Key Laboratory of Power Transmission Equipment &System Security and New Technology (Chongqing University), Chongqing, China, e-mail: laiweicqu@cqu.edu.cn
*Corresponding author.

$p_{Load\_i}(t)$	Active load demand at node i at time t (kW)
$q_{Load\_i}(t)$	Reactive load demand at node i at time t (kVar)
$p_{g,min}/p_{g,max}$	Min/max active power at PCC (kW)
$q_{g,min}/q_{g,max}$	Min/max reactive power at PCC (kVar)
$p_{i,min}/p_{i,max}$	Min/max active power of PV (kW)
$q_{i,min}/q_{i,max}$	Min/max reactive power of PV (kVar)
$p_{B,min}/p_{B,max}$	Min/max active power of DESS (kW)
$_{qB,min}/q_{B,max}$	Min/max reactive power of DESS (kVar)
$\Delta p_g(t)$	Active power ramp rate of PCC at time t, defined as $\Delta p_g(t) = p_g(t) - p_g(t-1)$
$\Delta p_i(t)$	Active power ramp rate of PV at time t, defined as $\Delta p_i(t) = p_i(t) - p_i(t-1)$
$\Delta p_{B,i}(t)$	Active power ramp rate of DESS at time t, defined as $\Delta p_{B,i}(t) = p_{B,i}(t) - p_{B,i}(t-1)$

1. Introduction

In March 2021, the Chinese government introduced the "30 • 60" dual-carbon policy [1], indicating that a new-type power system with new energy as the main body represents the future development direction of the power system. Guided by this policy, a large number of renewable energy sources have been integrated into the power system, the intermittent and stochastic nature of their output power has intensified grid power fluctuations while causing voltage amplitudes at certain nodes to exceed safety limits. This phenomenon adversely affects the normal operation of electrical equipment and poses significant risks to power consumption safety [2]. To effectively manage power grids, particularly in optimizing distributed generation output within LVDNs, achieving node voltage regulation and ensuring economical grid operation have emerged as critical research priorities.

Reactive power compensation methods [3-4] have demonstrated that reactive power control through voltage-reactive power (V-Q) controllers can effectively achieve voltage regulation in such distribution systems. Active and reactive power adjustment strategies [5-6] indicate that in distribution networks (DNs) where line resistance and reactance are approximately equivalent, both active and reactive power adjustments can effectively regulate voltage levels. In node voltage regulation methodologies, sensitivity matrix-based voltage regulation [7] is commonly used to deal with voltage regulation problems. Key grid assets utilized for voltage magnitude regulation include distributed generators employing active power curtailment techniques, capacitor bank switching, and energy storage system (ESS) power modulation [7]. Consequently, nodal voltages can be maintained within permissible ranges through coordinated renewable energy and capacitor control [8]. Addressing short-timescale voltage fluctuations, distributed energy storage system (DESS)-based regulation [9] proposes a sensitivity matrix approach to ensure voltage stability. Given the inherent correlation between nodal voltage variations and power flow losses, researchers have developed voltage-loss

integrated optimization [10] incorporating both voltage sensitivity and network loss considerations.

Centralized reactive power control frameworks optimize reactive power dispatch via coordinated optimization to achieve nodal voltage regulation. Robust optimization-based voltage regulation [11] minimizes distribution network (DN) operational costs through demand-response-based flexible load control, synergizing the reactive power capabilities of distributed energy resources with conventional voltage regulation devices. Furthermore, DG-OLTC coordinated control [12-13] incorporates power loss minimization objectives into the voltage regulation process, improving DN economic efficiency.

Power flow analysis indicates that nodal voltage variations depend on line power flow magnitudes and impedance characteristics. Under fixed power flow conditions: When line resistance significantly exceeds reactance (R>>X), voltage deviations predominantly depend on active power flow; When reactance dominates resistance (X>>R), voltage changes are mainly influenced by reactive power flow; For comparable R/X ratios, both active and reactive power flows jointly affect voltage profiles [14-15]. To maximize renewable energy integration, DESS-based power balancing schemes are proposed. This system absorbs surplus power during peak renewable generation periods and discharges during generation deficits to maintain power balance. Additionally, strategically deployed ESS can shorten power transmission paths, thereby reducing both network losses and voltage drops.

Existing research primarily focuses on single-objective voltage regulation strategies, such as reactive power compensation or active power curtailment, while neglecting the coordinated optimization of operational economy, renewable energy utilization, and voltage stability. Conventional strategies exhibit limitations in managing interactive active-reactive power dynamics within networks featuring comparable resistance-to-reactance ratios, resulting in inefficient resource utilization and recurrent voltage deviations. To bridge this gap, this paper proposes a multi-objective power optimization management model that innovatively integrates distributed PV systems and DESS for joint active-reactive power dispatch. The model uniquely incorporates four interdependent objectives: voltage deviation minimization, PV curtailment reduction, DESS lifetime preservation, and grid loss mitigation, all constrained by operational and equipment safety limits. By establishing a weighted optimization framework and validating it through a 21-node practical case study, this work demonstrates a coordinated control mechanism that ensures voltage security while maximizing renewable energy penetration — a critical advancement for low-voltage networks transitioning to high-PV scenarios.

2. Model of a LVDNs with Distributed PV and DESS

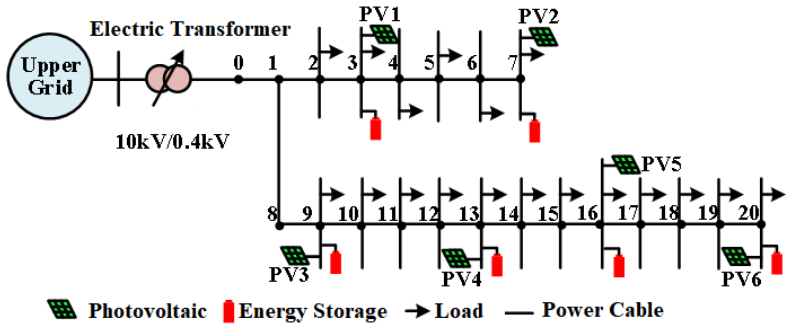

Fig. 1. LVDNs with distributed PV sources and DESS

Based on an actual engineering project, this section establishes a power management model for a 0.4 kV LVDNs with 21 nodes, as shown in Fig. 1. In this model, there are six distributed PV and six DESS, which are respectively connected to nodes 3, 7, 9, 13, 16, and 20 of the DN. The PV operates under the maximum power point tracking (MPPT) control mode, while the DESS work in the constant-power control mode.

2.1 Voltage optimization objective of LVDNs

According to the node voltage amplitude fluctuation equation in the linearized power flow equations proposed in References [16-17], the flow of reactive power and active power in the DN will cause line voltage losses. In severe cases, it may lead to voltage out - of - limit, which in turn results in abnormal operation of power equipment. The voltage amplitude of each node can be approximately expressed as:

$$\begin{aligned} P_{\mathrm{L},i} &= P_{\mathrm{L},i-1} - L_{R,i-1}\frac{P_{\mathrm{L},i-1}^2 + Q_{\mathrm{L},i-1}^2}{V_{i-1}^2} - P_i \\ Q_{\mathrm{L},i} &= Q_{\mathrm{L},i-1} - L_{X,i-1}\frac{P_{\mathrm{L},i-1}^2 + Q_{\mathrm{L},i-1}^2}{V_{i-1}^2} - Q_i \\ V_i^2 &= V_{i-1}^2 - 2\left(L_{R,i-1}P_{\mathrm{L},i-1} + L_{X,i-1}Q_{\mathrm{L},i-1}\right) \\ &\quad + \left(L_{R,i-1}^2 + L_{X,i-1}^2\right)\frac{P_{\mathrm{L},i-1}^2 + Q_{\mathrm{L},i-1}^2}{V_{i-1}^2} \end{aligned} \tag{1}$$

Where i represents the node index (ranging from 1 to N, where N is the total number of nodes in the network). Matrices L_R and L_X represent the matrices composed of the line resistance and reactance parameters, respectively. P and Q denote the vectors of the injected power at the nodes, while P_L and Q_L stand for the power flowing through the lines.

To address the issues of voltage violations and the efficient utilization of renewable energy, a voltage regulation model for the DN with regulated distributed PV systems and DESS is designed:

$$\min F_1 = \min_{P,Q} \sum_{i=1}^{N} \left| L_{R\_i} \cdot P + L_{X\_i} \cdot Q \right| \tag{2}$$

Where N represents the number of nodes, and L_{R_i} and L_{X_i} represent the i-throw vectors of matrices L_R and L_X, respectively. The role of the objective function F_1 is to minimize the voltage deviation of the system by adjusting P and Q, that is, to minimize the system voltage loss. Vectors P and Q contain the power of all adjustable units, including the power of distributed PV systems, DESS, and the power exchanged with the main grid.

2.2 Objective of Renewable Energy Power Curtailment Reduction

To enhance the power generation capacity of distributed PV sources and minimize the active power curtailment, the objective function F_2 is formulated as:

$$\min F_2 = \min_{p_i, q_i} \sum_{i=1}^{M_1} \left(p_i(t) - p_{i\_ref}(t) \right)^2 + \left(q_i(t) \right)^2 \tag{3}$$

Where M_1 denotes the total number of distributed PV sources;the index i here refers only to nodes with installed PV systems (ranging from 1 to M1, distinct from the node index i in Equation (1) which covers all nodes in the network, $i \in \{3,7,9,13,16,20\}$ in this model).$p_i(t)$ and $q_i(t)$ represent the distributed PV output active and reactive power at time t; pi-ref(t) is the forecasted active power value of the PV source at time t.

$p_i(t)$ and $q_i(t)$ represent the distributed PV output active and reactive power, and $p_{i\text{-}ref}(t)$ is the forecasted active power value of the PV source.

2.3 Objective for DESS and Grid-Coupled Node

To prolong the lifespan of the DESS and minimize its output and absorption power as much as possible, the objective function F3 for the DESS and the grid-connected coupling node is designed as follows:

$$\min F_3 = \min_{p_g, q_g, q_B} \left[\left(p_g(t) \right)^2 + \left(q_g(t) \right)^2 + \left(\sum_{i=1}^{N_B} (q_{B,i}(t)^2 + p_{B,i}(t)^2) \right) \right] \tag{4}$$

Where t represents the time variable within the scheduling period; $pB,i(t)$ and $q_{B,i}(t)$ denote the active and reactive power output of the i-th DESS at time t; $p_g(t)$ and $q_g(t)$ denote the active and reactive power at the point of common coupling (PCC) node at time t.

2.4 Grid Power Loss Objective

To minimize power transmission losses in the power grids, the power loss objective function is considered in the optimal management of distributed energy resources (DERs), and it is given by Equation (5):

$$\begin{aligned} F_4 &= \min \sum_{t=1}^{T} P_{\text{loss-total}}(t) \\ &= \min \sum_{t=1}^{T} \sum_{i=1}^{n} \left(L_{R,i-1}^2 + L_{X,i-1}^2 \right) \frac{P_{\text{L},i-1}^2(t) + Q_{\text{L},i-1}^2(t)}{V_{i-1}^2(t)} \end{aligned} \tag{5}$$

Where t is the time index (t=1, 2, ⋯,T); T is the total scheduling period (24 hours); $V_i(t)$ is the voltage magnitude at node i at time t.The line loss power depends on line parameters, L_R,L_X and node voltage magnitudes V_i. By optimizing the power injection at nodes, the branch power flow can be dynamically adjusted, thereby adjusting the line loss power.

2.5 Constraints

The above three objective functions are subject to the following constraints: output power limits of DESS, state of charge (SoC) limits, power limits of distributed PV sources, power balance constraints, and ramping rate constraints of power source outputs. These constraints are categorized into active power constraints (Equation 6) and reactive power constraints (Equation 6'), in which NB and M1 represent the number of DESS and distributed PV. Symbol definitions are provided in Table 1.

$$\begin{cases} p_{g\_\min} \le p_g(t) \le p_{g\_\max} \\ p_{i\_\min} \le p_i(t) \le p_{i\_\max}, i \in M_1 \\ p_{B\_\min} \le p_{B,i}(t) \le p_{B\_\max} \\ \sum_{t=1}^{T} p_{B,i}(t)\Delta t = 0, \qquad i = 1,\cdots,N_B \\ \sum_{i=1}^{N_B} p_{B,i}(t) + \sum_{i=1}^{M_1} p_i(t) + p_g(t) = \sum_{i=1}^{N} p_{Load\_i}(t), \quad t = 1,\cdots,T \\ \Delta p_{g\_\min} \le \Delta p_g(t) \le \Delta p_{g\_\max}; \;\; \Delta p_{i\_\min} \le \Delta p_i(t) \le \Delta p_{i\_\max}, i \in M_1 \\ \Delta p_{B\_\min} \le \Delta p_{B,i}(t) \le \Delta p_{B\_\max} \end{cases} \tag{6}$$

By replacing the symbol 'p' with 'q' in Constraint (6), the reactive power constraints emerge directly by equation (6').

$$\begin{cases} q_{g\_\min} \le q_g(t) \le q_{g\_\max} \\ q_{i\_\min} \le q_i(t) \le q_{i\_\max}, i \in M_1 \\ q_{B\_\min} \le q_{B,i}(t) \le q_{B\_\max} \\ \sum_{i=1}^{N_B} q_{B,i}(t) + \sum_{i=1}^{M_1} q_i(t) + q_g(t) = \sum_{i=1}^{N} q_{Load\_i}(t), \quad t = 1,\cdots,T \end{cases} \tag{6'}$$

In summary, through the weighting method, the above-mentioned multi-objective optimization problem is transformed into a single-objective optimization

problem, and a power management model for LVDNs with distributed PV systems and DESS is obtained as follows:

$$\begin{cases} \min\limits_{P,q} \dfrac{1}{4}\left(F_1+F_2+F_3+F_4\right) \\ S.t \quad \text{Equation (6) (active power constraints)} \\ \qquad \text{Equation (6') (reactive power constraints)} \end{cases} \tag{7}$$

2.6 Clarification on Operational Conditions of the LVDN

To clarify the operational context of the proposed low-voltage distribution network (LVDN) model, the following points are addressed based on the system setup and assumptions:

①Sizing of Renewable Sources: The distributed photovoltaic (PV) systems are sized not only to cover local load demand but also to allow for active power injection into the upstream grid. As indicated in Section 4.1, the total installed PV capacity (350 kW) significantly exceeds the maximum local load demand (approximately 100 kW), enabling both local consumption and surplus power export.

②Intervention at MV/LV Transformer: The proposed control strategy focuses on the coordination of distributed energy resources within the low-voltage network. No active interventions (e.g., tap changing) at the MV/LV power transformer are considered in this study, as voltage regulation is achieved solely through the coordinated dispatch of PV inverters and distributed energy storage systems (DESS).

③Inverter Voltage Limitation: The PV inverters operate under maximum power point tracking (MPPT) control mode without explicit maximum voltage limitation functionality. Voltage violations are mitigated through the proposed optimization-based power management strategy, which adjusts active and reactive power outputs rather than relying on local inverter protection mechanisms.

④Data Accessibility for Network Operator: The optimization model assumes that the network operator has full access to real-time measurement and control data from all nodes with distributed resources (PV and DESS), as well as the point of common coupling (PCC). This is implicit in the centralized optimization framework implemented in MATLAB.

⑤Availability of Energy Storage: The low-voltage network operator has control over six distributed energy storage systems (DESS) installed at nodes 3, 7, 9, 13, 16, and 20. These are used for active and reactive power support to maintain voltage stability and optimize system operation.

3. Optimization Method and System Parameter Settings

3.1 Optimization Method and Implementation

To solve the multi-objective optimization model established in Section 2, a weighted sum method is adopted to convert the multi-objective problem (Equation 7) into a single-objective optimization problem. The weights of the four objectives (F_1-F_4) are determined through analytic hierarchy process (AHP), considering the priority of voltage stability and renewable energy utilization in low-voltage distribution networks (LVDNs). The specific weight values are set as ω_1=0.4, ω_2=0.3, ω_3=0.15, ω_4=0.15, which are validated through sensitivity analysis to ensure robustness.

The optimization process is implemented in MATLAB [18], using the interior-point algorithm for solving the constrained nonlinear programming problem. The algorithm iteratively adjusts the decision variables (active/reactive power of PV, DESS, and PCC node) to minimize the weighted objective function, while satisfying the constraints in Equations (6) and (6'). The key steps are as follows:

①Initialization: Set the initial values of decision variables, including SoC of DESS (50% at t=0) and initial power outputs of PV (MPPT mode).

② Objective Function Calculation: Compute F_1-F_4 based on current variables and system states.

③Constraint Check: Verify if all active/reactive power constraints, SoC limits, and ramping rates are satisfied.

④Optimization Iteration: Use the interior-point method to update decision variables, adjusting step sizes based on constraint violations to ensure convergence.

⑤Convergence Criterion: Terminate iteration when the change in objective function value between consecutive steps is less than 1e-6 or the maximum iteration number (500) is reached.

3.2 System Parameter Settings for Case Study

The optimization method is validated on a 21-node 0.4kV LVDN (Fig. 1) derived from an actual engineering project. In this network, distributed PV power sources and DESS are installed at nodes 3, 7, 9, 13, 16, and 20, respectively. The line parameter is Z=0.335+j0.06Ω/km, and the total length of the power supply line is 2.16 km. The load nodes are located at nodes 2, 3, 4, 6, 9, 10, 12, 13, 16, 17, and 19. Each load node represents an electricity consumer or a large - scale electrical load. The simulation period is set to 96 cycles, with each cycle lasting 15 minutes. That is, sampling is performed every 15 minutes. A scheduling period is 24 hours, denoted as T=24h.

4. Simulation Case Study

4.1 Fluctuations in Load and Renewable Power Generation

When the DN is not managed, the nodal load demand, renewable power generation data, and voltage conditions are shown in Fig. 2(a), (b), and (c), respectively. As shown in Fig. 2, the nodal load varies between 50 and 100 kW, with a maximum load variation of approximately 50 kW. From Fig. 2(a), the system load demand is relatively high during 6:00–8:00, 11:00–13:00, and 18:00–22:00, fluctuating between 75 and 100 kW. During other periods, the load ranges from 50 to 75 kW, which is consistent with residential electricity consumption patterns. The power output of distributed PV systems correlates with solar irradiance, and the total peak power of the distributed PV systems reaches 350 kW. The total installed PV capacity (350 kW) significantly exceeds the maximum grid load (~100 kW), allowing for both local consumption and active power injection to the upstream grid, which indicates that the PV systems are not sized solely for self-consumption. Between 6:00 and 19:00, the active power output of the PV systems increases with solar irradiance, reaching its peak around 14:00. At 7:00, the PV power output power matched the grid load demand. Subsequently, as solar irradiance gradually increased, the PV generation exceeded the load demand, resulting in surplus power being fed into the upstream grid. After 17:30, the PV power output gradually becomes insufficient to meet the load demand.

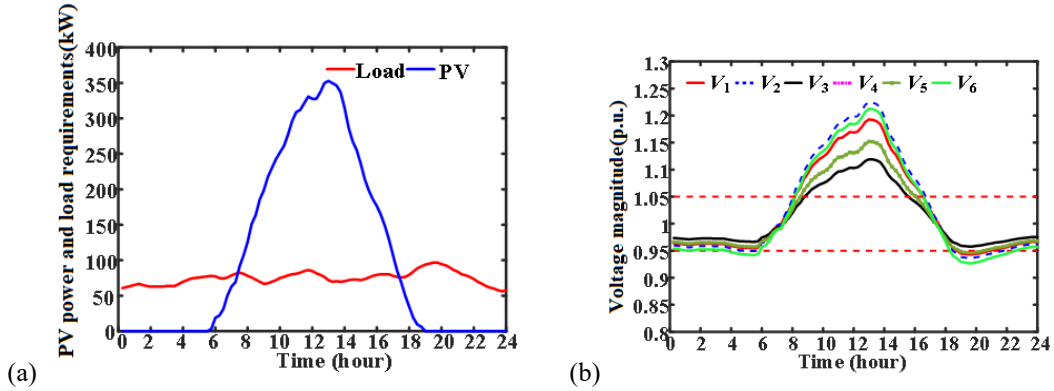

(a) (b)

Fig. 2. The Figs will have a centered legend (10 pts)Load demand, nodal voltages and PV power outputs of DN (a) Total grid load demand and PV power generation; (b) Voltage magnitude variation at PV grid-connected nodes.

Since the output power of the PV power exceeds the load demand, the node voltage amplitude exceeds the upper limit of the voltage safety range, leading to the node voltage violation behavior, as specifically shown in Fig. 2(b). During the period from 08:00 to 16:00, the voltage magnitudes at PV grid-connected nodes exceeded the safety upper limit, with the peak voltage magnitude reaching 1.22 per unit (p.u.).

The active power injection from PV systems leads to a significant rise in nodal voltage magnitudes, which severely compromises the safe operation of electrical equipment. Furthermore, partial PV inverters may disconnect from the grid due to the activation of protection mechanisms, resulting in grid connection failures and curtailment of PV power absorption. Therefore, it is imperative to implement active power optimization management in DNs with high-penetration distributed PV systems.

4.2 Operational Results without Considering Nodal Voltage Objectives and Constraints

When the power optimization management model for the DN proposed in Section 3 is adopted, but the voltage loss objective and nodal voltage constraints are not considered, the power of distributed PV sources and DESS is adjusted. The simulation results are shown in Fig. 3.

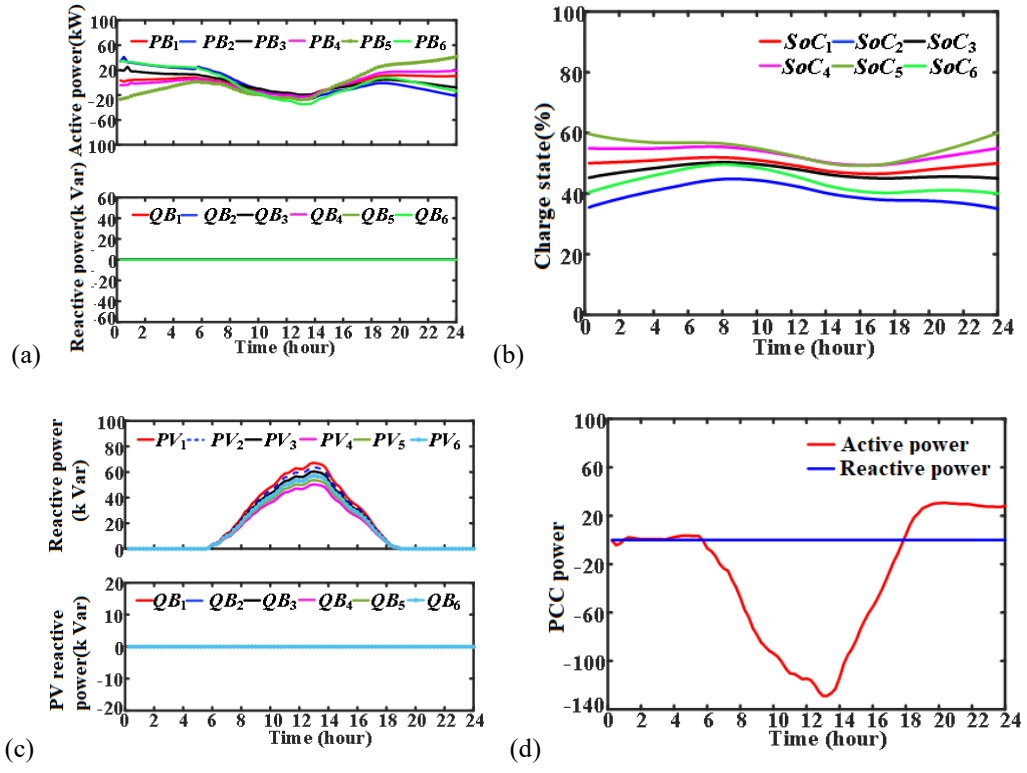

Fig. 3. Simulation results of the DN without considering voltage objectives and constraints (a) power of DESS; (b) SoC of DESS; (c) Output power of distributed PV; (d) power at Grid PCC node.

As observed in Fig. 3(a), the active power of the DESS fluctuates between −40 kW and 40 kW, while its reactive power output remains zero. Simultaneously, the SoC of the DESS fluctuates between 35% and 60% during operation. At the last scheduling interval, the SoC is restored to its initial value under the energy balance constraint, as shown in Fig. 3(b).

The power output of the nodal distributed PV systems is depicted in Fig. 3 (c), indicating that the active power ranges from 0 to 70 kW, while the reactive power output is consistently maintained at zero. The power variations at the grid's PCC are illustrated in Fig. 3 (d). Owing to the surplus power from the PV systems, the active power injection at the PCC is greater than 100 kW, while the reactive power remains zero.

The fluctuation of nodal voltage magnitudes is demonstrated in Fig. 4, where the voltage magnitudes vary between 0.95 and 1.1 p.u. Notably, when the PV power surpasses the load demand, the voltage magnitudes progressively increase and breach the upper safety limit. Therefore, when the nodal voltage constraints and objectives are not considered, the nodal voltage magnitudes exceed the limits severely.

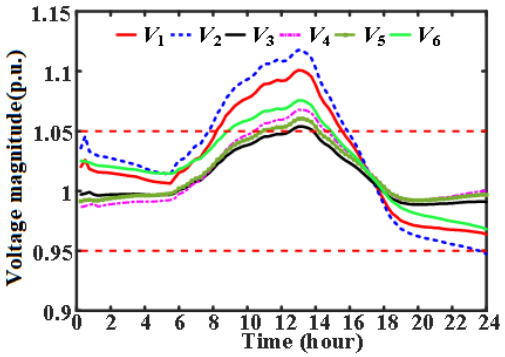

Fig. 4. Fluctuation of nodal voltage magnitudes.

4.3 Operational Results Considering Nodal Voltage Objectives and Constraints

When voltage loss objective and nodal voltage constraints are considered, the simulation results of the DN are shown in Fig. 5. As shown in Fig. 5(a), the active power of the DESS varies between -50 kW and 30 kW, while its reactive power output fluctuates between -25 kVar to 0 kVar. Concurrently, the SoC of the DESS ranges from 30% to 60%. Furthermore, under the energy balance constraint, the SoC of the DESS returns to its initial value at the last scheduling interval, as specifically illustrated in Fig. 5(b).

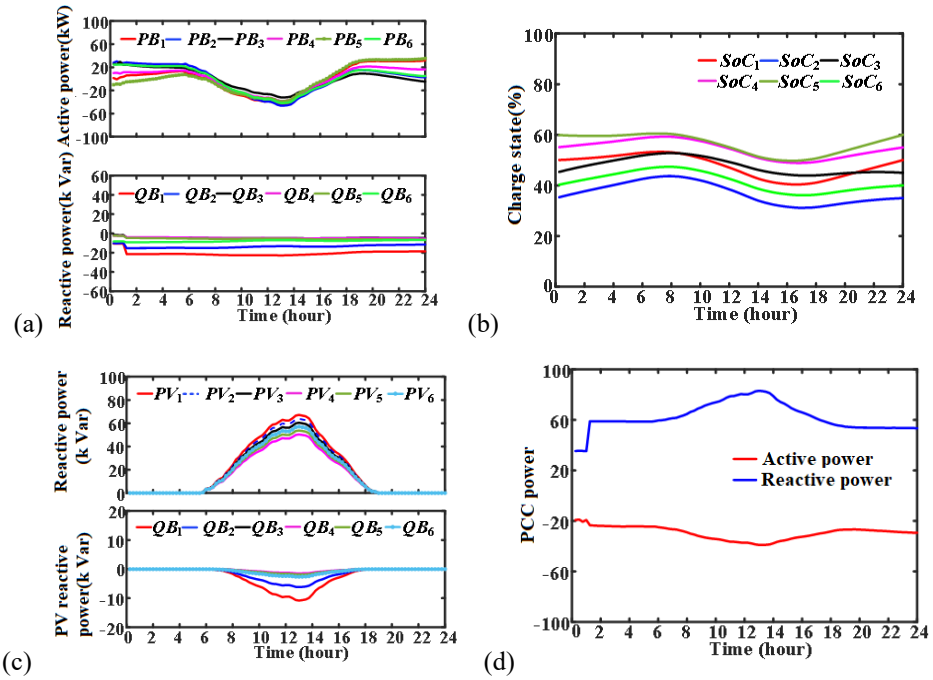

Fig. 5. Simulation results of the DN considering voltage objectives and constraints (a) power of DESS; (b) SoC of DESS; (c) Output power of distributed PV; (d) power at Grid PCC node.

The power output of distributed PV at the nodes is depicted in Fig. 5(c). The active power output of the PV varies from 0 kW to 70 kW, while their reactive power output fluctuates between -15 kVar and 0 kVar. Reactive power is generated by the PV when their output exceeds load demand. Owing to the active power objective of the PV system, the actual output matches the predicted value, thereby achieving MPPT operation. As illustrated in Fig. 5(d), the active power injection at the PCC node is maintained within the range of -40 kW to -20 kW as a result of surplus power generated by the PV sources. Meanwhile, the reactive power varies within 30 – 80 kVar to regulate the nodal voltage amplitude.

Under the combined effects of nodal voltage constraints and optimization objectives, the voltage magnitudes at all nodes fluctuate within the normal operating range, as illustrated in Fig. 6.

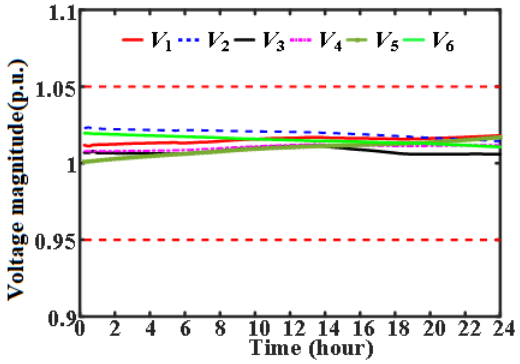

Fig. 6. Fluctuation of nodal voltage magnitudes.

4.4 Operational Results Considering the Reactive Power Optimization Objective

In the above results, the operational objective of reactive power was not taken into account, that is, the reactive power injection was not minimized. In this section, to reduce the cost of reactive power compensation and decrease the reactive power injection, the objective of minimizing reactive power is introduced into the management model. The results obtained are shown in Fig. 7. It can be seen that the reactive power outputs of both the DESS and the PV remain zero. The changes in the active power of the energy storage system and the PV sources are similar to the results in Section 4.3. The active power at the PCC node varies between -40 kW and -20 kW, which is similar to that in Fig. 5(d). However, the reactive power at the PCC node remains constant at zero.

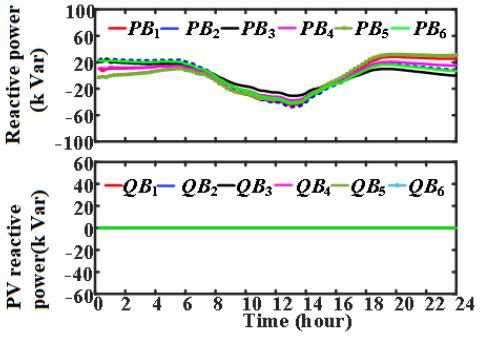

(a)

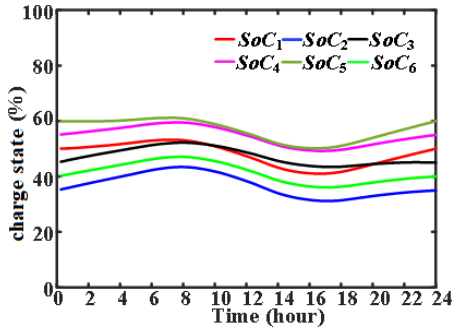

(b)

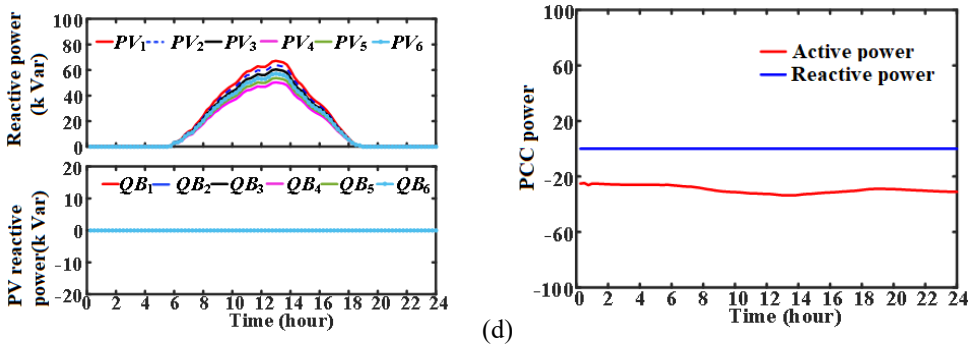

(c) (d)

Fig. 7. Operational results of the DN after introducing the reactive power optimization into the management model (a) power of DESS; (b) SoC of DESS; (c) Output power of distributed PV; (d) power at Grid PCC node.

In addition, the node voltage magnitudes can still be maintained within the normal range, as illustrated in Fig. 8. Consequently, the nodal voltage regulation problem can be resolved by adjusting the active power of the DESS. This approach avoids reactive power injection, thereby reducing the cost of reactive power compensation.

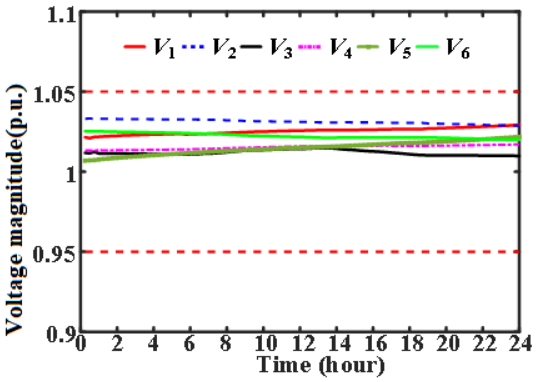

Fig. 8. Fluctuation of nodal voltage magnitudes.

5. Conclusions

For LVDNs with high-penetration distributed PV integration, this study proposes a power management strategy based on coordinated dispatch of DESS and PV units. By jointly regulating active and reactive power outputs, the strategy achieves nodal voltage stabilization and economic grid operation. Simulation results demonstrate that the proposed method effectively reduces voltage deviations while maintaining system voltages within safe operating ranges. Case studies under various scenarios further confirm that active power coordination between DESS and PV systems enables nodal voltage regulation while minimizing reactive power

compensation requirements — offering a practical solution for enhancing operational efficiency in LVDNs.

Acknowledgements

This research was funded by the major project of science and technology research program of Chongqing Education Commission of China, grant number KJZD-M202402401.

REFERENCES

[1]. Liu, Y., Zhang, X., & Wang, J. (2022). China's "30·60" carbon goals: Pathways for building a renewable-dominated power system. Applied Energy, 318, 119235.

[2]. Guodong, C. Wenhao. (2024) "Photovoltaic power prediction based on improved pyraformer". U.P.B. Sci. Bull., Series C, vol. 86, no. 1, 385-398.

[3]. Almeida, D.; Pasupuleti, J.; Ekanayake, J. Comparison of Reactive Power Control Techniques for Solar PV Inverters to Mitigate Voltage Rise in Low-Voltage Grids. Electronics 2021, 10(13), 1569.

[4]. Zhang, Y.; Liu, J.; Li, Z.; Wang, C. Reactive Power Optimization in Low-Voltage Distribution Networks with High Penetration of Photovoltaic Systems. Energies 2023, 16(13), 5123

[5]. Sasi Bhushan, M.A.; Sudhakaran, M.; Dasarathan, S.; E, M. Integration of a Heterogeneous Battery Energy Storage System into the Puducherry Smart Grid with Time-Varying Loads. Energies 2025, 18(2), 428

[6]. Župan, I.; Šunde, V.; Ban, Ž.; Novoselnik, B. Regenerative Braking Energy Flow Control Algorithm for Power Grid Voltage Stabilization in Mobile Energy Storage Systems. Energies 2025, 18(2), 410

[7]. Luo, Y.; Chen, M.; Kang, W.; Li, C. Distributed Event-Triggered Voltage Control with Limited Reactive Power in Low Voltage Distribution Networks. Electronics 2021, 10, 128.

[8]. Bolognani, S.; Carli, R.; Cavraro, G.; Zampieri, S. Distributed Reactive Power Feedback Control for Voltage Regulation and Loss Minimization. IEEE Trans. Autom. Control 2015, 60, 966-981.

[9]. Cai, Y.X.; Tang, W.; Zhang, B.; Li, P. Including a High Proportion of Household Photovoltaic Low-Voltage Distribution Network Centralized-Local Two-Stage Voltage-Reactive Power Control. Power Syst. Technol. 2019, 43, 1271-1280.

[10]. A. G. Madureira, J. A. Pecas Lopes, "Centralized Reactive Power Control for Voltage Regulation in Distribution Networks with High DG Penetration", IEEE Transactions on Sustainable Energy, vol. 14, no. 2, pp. 1045-1056, Apr. 2023.

[11]. M. A. Hussain, S. H. Low, "Robust Voltage Regulation in Active Distribution Networks via Demand Response and Distributed Energy Resources Coordination", IEEE Transactions on Power Systems, vol. 38, no. 3, pp. 2291-2303, May 2023.

[12]. G. Valverde, D. E. Olivares, "Coordination of Distributed Generation and OLTC for Joint Voltage Regulation and Loss Minimization", Electric Power Systems Research, vol. 221, pp. 109432, Oct. 2023.

[13]. A. J. Conejo, M. Carrion, "Robust Optimization-Based Voltage Control for Distribution Networks with OLTC and Photovoltaic Systems", International Journal of Electrical Power & Energy Systems, vol. 142, pp. 108321, Sep. 2023.

[14]. A. A. Eajal, M. F. Shaaban, E. El-Saadany, "A Unified Approach for Voltage Sensitivity Analysis in Distribution Networks with High R/X Ratios", IEEE Transactions on Power Systems, vol. 5, no. 5, Sep. 2020, pp. 3620-3633.

[15]. M. A. Hossain, H. R. Pota, S. Squartini, "Two-Stage Energy Storage Dispatch Framework for Power Balance Maintenance in High-Penetration PV Systems", Applied Energy, vol. 304, Dec. 2021, pp. 117803.
[16]. S. Mishra, D. K. Mishra, "Optimal Siting of ESS in Radial Distribution Networks for Simultaneous Loss Minimization and Voltage Profile Improvement", International Journal of Electrical Power & Energy Systems, vol. 135, no. 2, Feb. 2022, pp. 107542.
[17]. Wei, C.; Li, Q.; Chen, M.; Li, G.; Guo, Y. Power-Mileage-Based Algorithm for the Optimization of Distribution Network Structures via Adding Transmission Lines. Energies 2019, 12, 1623.
[18]. Dobrea, M. A., Vasluianu, M., Neculoiu, G., & Arghira, N. (2021). "Modeling and simulation of a 3 kW photovoltaic system for an autonomous consumer". U.P.B. Sci. Bull., Series C, vol. 83, no. 2, 35-46.